JOURNAL OF THERMOPHYSICS AND HEAT TRANSFER
Vol. 13, No. 1, January–March 1999

Experiment–Modeling Comparison in a Nonequilibrium Supersonic Air Nozzle Flow

A. Bourdon,* A. Leroux,† P. Domingo,* and P. Vervisch‡
Université de Rouen, 76821 Mont Saint Aignan CEDEX, France

The modeling of a supersonic air nozzle flow is presented and compared with measurements at the nozzle exit. Shortcomings of state-of-the-art models for the kinetic scheme and energy exchange terms are discussed. In particular, the significant influence of an accurate modeling of vibrational–translational and vibrational–vibrational energy exchanges is shown. Conversely, the choice of the model for the kinetic scheme and for the chemical–vibrational energy exchange term only has a small influence on the results.

Nomenclature

A_s = name of the sth species
c_v = mass-averaged specific heat at constant volume J/(kg K)
$D_{s,\mathrm{mix}}$ = effective diffusion coefficient of species s in the mixture, m^2/s
d_s = collision diameter of species s, m
e_c = kinetic energy per unit mass, J/kg
e_t = total energy per unit mass, J/kg
e_{v_m} = vibrational energy of molecule m per unit mass, J/kg
$\bar{e}_{v_m}$ = vibrational energy of molecule m, J/mol
$e_{v_m}(T)$ = vibrational energy of molecule m at local T, J/kg
k_B = Boltzmann constant, J/K
h_s = enthalpy of species s per unit mass, J/kg
h_s^0 = heat of formation of species s per unit mass, J/kg
$k_{1,0}^{m,k}$ = exothermic vt rate coefficient between molecule m and species k for the process: $A_m(v = 1) + A_k \rightarrow A_m(v = 0) + A_k$, m^3/s
$\mathcal{M}_r$ = molar mass of species r, kg
$\mathcal{N}_A$ = Avogadro number
P_{mr} = vv exchange probability for molecules m and r
p = pressure, Pa
Q_{cv_m} = chemical–vibrational energy exchange term for molecule m, W/m^3
Q_{vt_m} = vibrational–translational energy exchange term for molecule m, W/m^3
Q_{vv_m} = vibrational–vibrational energy exchange term for molecule m, W/m^3
q_j = total heat flux in the j direction, W/m^2
q_{tr_j} = translational–rotational heat flux in the j direction, W/m^2
$q_{v_{m_j}}$ = vibrational heat flux of molecule m in the j direction, W/m^2
T = translational–rotational temperature, K
$T_{v,m}$ = vibrational temperature of molecule m, K
u_i = mass-averaged velocity in the i direction, m/s
u_{s_j} = diffusion velocity of species s in the j direction, m/s
$\dot{w}_{\mathrm{app},mj}$ = mass production rate of molecule m in the reaction j, kg/(m^3 s)
$\dot{w}_s$ = mass source term of species s, kg/(m^3 s)
$\dot{w}_{va,mj}$ = mass decomposition rate of molecule m in the reaction j, kg/(m^3 s)
θ_s = characteristic vibrational temperature of species s, K
λ_n = thermal conductivity of the gas mixture for the energy mode n, W/(m K)
μ_{mr} = reduced mass of species m and r, kg
ρ = sum of the species densities, kg/m^3
ρ_s = density of species s, kg/m^3
σ_{mr} = $d_m d_r$, collision cross section of species m and r, m^2
τ_{ij} = viscous stress tensor, kg/(m s^2)
τ_{vt_m} = global vt relaxation time of molecule m, s

Received Feb. 27, 1998; revision received Sept. 8, 1998; accepted for publication Oct. 12, 1998.

*Research Scientist, Unité Mixte de Recherche No. 6614.
†Postdoctorate Fellow, Unité Mixte de Recherche No. 6614; currently at Eindhoven University of Technology, Department of Applied Physics, P.O. Box 513, 5600 MB Eindhoven, The Netherlands.
‡Senior Scientist, Unité Mixte de Recherche No. 6614.

I. Introduction

To simulate, in ground facilities, the real environment of space vehicles, supersonic flows are generated by expanding high-enthalpy gases through converging–diverging nozzles. At the outlet, the flow is generally in strong thermochemical nonequilibrium (vibrationally excited, dissociated, and even ionized). Then, temperatures and densities behind the shock formed around a test model located downstream of the nozzle exit are affected by the energy contained in these real-gas modes. Thus, to obtain the upstream conditions of the test model, an accurate prediction of the nozzle flowfield is necessary. In this work, we propose to study the airflow in the nozzle of the TT1 facility located at Tsniimach (Moscow). TT1 is a 10-MW arcjet facility built for material testing. Its nozzle is axisymmetric and contoured. A thorough experimental investigation has been carried out in this facility[1]: NO number density, velocity, and NO rotational temperature have been measured using the laser-induced fluorescence technique over different test samples and in a 40-mm-wide and 40-mm-long freejet volume located 170 mm downstream of the nozzle exit. Recently, Tumino et al.[2] computed the flow in the TT1 nozzle with widely used thermochemical models (one average vibrational temperature for all molecules, Millikan and White's[3] relaxation times for the vibration–translation coupling, and Dunn and Kang's[4] chemical model with the two-temperature model proposed by Park[5]). These authors pointed out that the influence of viscous effects, turbulence, and wall conditions on the flow conditions on the nozzle axis is small. As in the study of the F4 hot-shot wind tunnel,[6] significant discrepancies between computations and experiments are observed. The objective of this work is to study the influence of a more accurate modeling of the kinetic scheme, vibrational–vibrational (V–V), vibrational–translational (V–T), and chemical–vibrational (C–V) energy exchange terms on the experiment/modeling agreement at the TT1 nozzle exit. In Sec. II, the governing equations and boundary conditions are given. Then the physical and chemical models are presented. Finally, the compari-

son between computations and experimental results is discussed.

II. Problem Formulation

A. Governing Equations

Five species are taken into account: N_2, O_2, NO, N, and O, and the three molecules are assumed to be a priori in thermal nonequilibrium. The equations that describe a flow in thermochemical nonequilibrium have been developed by Lee.[7] The mass-averaged momentum equation is

$$\frac{\partial \rho u_i}{\partial t} + \frac{\partial}{\partial x_j}(\rho u_i u_j) + \frac{\partial p}{\partial x_i} - \frac{\partial \tau_{ij}}{\partial x_j} = 0 \tag{1}$$

The mass conservation equation for each species s is

$$\frac{\partial \rho_s}{\partial t} + \frac{\partial}{\partial x_j}[\rho_s(u_j + u_{s_j})] = \dot{w}_s \tag{2}$$

The vibrational energy conservation equation for each type of molecule m is

$$\frac{\partial}{\partial t}(\rho_m e_{v_m}) + \frac{\partial}{\partial x_j}[\rho_m e_{v_m}(u_j + u_{m_j}) + q_{v_{m_j}}] = Q_{cv_m} + Q_{vt_m} + Q_{vv_m} \tag{3}$$

Finally, the overall energy conservation equation is

$$\frac{\partial \rho e_t}{\partial t} + \frac{\partial}{\partial x_j}[(\rho e_t + p)u_j - \tau_{ij}u_i + q_j] = 0 \tag{4}$$

with

$$\rho e_t = \rho c_v T + \sum_{m=1}^{3} \rho_m e_{v_m} + \sum_{s=1}^{5} \rho_s h_s^0 + \rho e_c \tag{5}$$

where the subscript s represents one of the five species, and m represents one of the three molecules.

B. Numerical Method and Computational Grid

The governing equations are solved using a finite volume approach. The second-order upwind non-MUSCL total variation diminishing scheme, proposed by Harten,[8] is used for nonviscous fluxes, and a second-order central difference scheme is used for viscous fluxes. The scheme is implicit, using Gauss–Seidel line relaxation. The geometry is axisymmetric. Figure 1 shows the computational domain. The throat is located at $x = 0$, where the diameter is 40.6 mm. The converging ($x < 0$) and diverging ($x > 0$) portions of the nozzle are 250 mm and 1553 mm long, respectively. One-hundred forty-two mesh points were used in the x direction, and 60 points were used in the y direction. The grid is stretched in the y direction to resolve the boundary layer that is particularly thin near the throat. Grid resolution studies have confirmed that the grid is sufficiently fine.

C. Boundary Conditions

The air mass flow rate and the arcjet electric power supply in the arc chamber have been measured, and are 0.5 kg s^{-1} and 4 MW, respectively. In the arc chamber, the measured pressure P_0 is 7 bar, and the temperature T_0 = 4160 K is derived from the pressure ratio P_0/P_{cold}, where P_{cold} is the pressure in the arc chamber when the arc is off. The distance between the electrodes and the converging part of the nozzle is long enough (220 mm) to assume that the flow is in thermochemical equilibrium at the nozzle inlet. In our calculations, the outlet of the nozzle is supersonic. The different variables

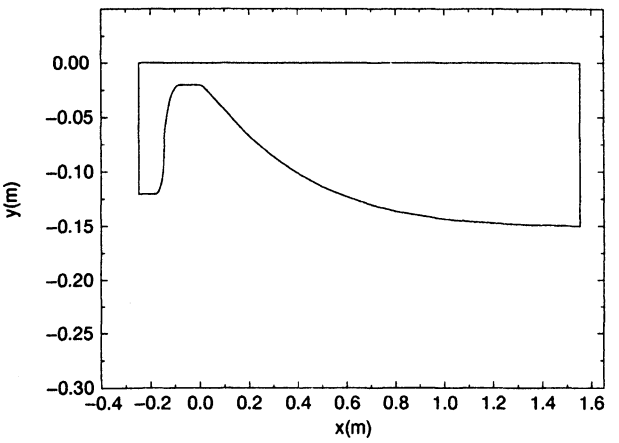

Fig. 1 Computational domain.

at the nozzle exit are obtained assuming a zero-gradient condition. On the symmetry axis, a zero-gradient condition is used for every variable except for the radial velocity component, which vanishes. At the wall, a no-slip condition is used for velocity. As in the work of Tumino et al.,[2] the wall is assumed to be either adiabatic or isothermal for the translational temperature, and noncatalytic. As the nozzle wall is metallic, the latter condition seems rather unrealistic and its influence on the results will be addressed in the following sections. For vibrational temperatures, a previous study[9] has shown that on a metallic wall, an adiabatic condition for vibration should be used.

III. Transport Properties

The viscous stress tensor τ_{ij} is given by

$$\tau_{ij} = \mu\left(\frac{\partial u_i}{\partial x_j} + \frac{\partial u_j}{\partial x_i}\right) - \frac{2}{3}\mu\delta_{ij}\,\text{div}\,\boldsymbol{v} \tag{6}$$

where μ, the viscosity of the mixture, is derived from Wilke's mixing law.[10] Viscosities of pure species are given by Gupta et al.[11]

The total heat flux q_j is

$$q_j = q_{tr_j} + \sum_{m=1}^{3} q_{v_{m_j}} + \sum_{s=1}^{5} \rho_s h_s u_{s_j} \tag{7}$$

The heat fluxes are assumed to be given by Fourier's heat law

$$q_{n_j} = -\lambda_n \frac{\partial T_n}{\partial x_j} \tag{8}$$

where n represents one of the energy mode (tr, v). Mason and Saxena's mixing law[12] has been used to determine the translational thermal conductivity of the mixture. The rotational and vibrational thermal conductivities are derived from an Eucken relation.

With Fick's law, the diffusion flux of species s in the j direction is

$$\rho_s u_{s_j} = -\rho D_{s,\text{mix}} \frac{\partial Y_s}{\partial x_j} \tag{9}$$

where $D_{s,\text{mix}}$ is given by a molar average mixing law.[13] The simplicity of Fick's law is very attractive, but it is an inconsistent model in the sense that the approximate diffusion fluxes do not properly sum to zero. Therefore, in this study, the self-consistent effective binary diffusion approximation proposed

by Ramshaw[14] has been used, with the binary diffusion coefficients given by Gupta et al.[11]

IV. Thermochemical Model

A. Kinetic Scheme

For dissociated air, the following reactions are considered:

$$N_2 + M \rightleftharpoons 2N + M \quad (R1)$$

$$O_2 + M \rightleftharpoons 2O + M \quad (R2)$$

$$NO + M \rightleftharpoons N + O + M \quad (R3)$$

$$NO + O \rightleftharpoons N + O_2 \quad (R4)$$

$$N_2 + O \rightleftharpoons N + NO \quad (R5)$$

where M is one of the five species. Two different models have been tested for the reaction rates. As a reference, we have considered Park's model,[15] which is widely used. Second, we have tested the reaction set proposed by Krivonosova et al.,[16] which will be denoted Losev's model in the following sections. For the vibration–chemistry coupling, the two-temperature model developed by Park[15] is widely used. However, the parameters of this model vary, depending on the problem under study, and this approach has been mainly tested for flows undergoing compression. Therefore, first, as a reference, we have used a one-temperature model: namely, all rate coefficients are calculated using the translational temperature T. Second, we have used the physically consistent coupled vibration–chemistry–vibration (CVCV) model proposed by Knab et al.,[17] which is an extension of the one developed by Treanor and Marrone[18] for dissociation reactions.

B. Energy Exchange Terms

1. V–T Energy Exchange Terms

The Landau–Teller relaxation equation is used

$$Q_{vt_m} = \rho_m \frac{e_{v_m}(T) - e_{v_m}(T_{v_m})}{\tau_{vt_m}} \quad (10)$$

where the global relaxation time τ_{vt_m} is derived from the interspecies relaxation times on the basis of a simple molar-averaged relation. For interspecies relaxation times, two sets have been tested: as a reference, Millikan and White's expressions[3] have been used. However, for the cases where the molecule is NO or the colliding species is an atom, Millikan and White's expressions are well known to overestimate relaxation times.[19] Therefore, we have tried to determine in the literature the best possible relaxation times. The second set used in this study is based on different studies,[9,20–23] but mainly on the review carried out by Doroshenko et al.,[20] and, therefore, this model will be referred to as Doroshenko's model in the following sections. Often in the literature, information is given on elementary exothermic V–T rate coefficients $k_{1,0}^{m,k}$ between molecule m and species k. The interspecies relaxation time $\tau_{m,k}^{vt}$ is related to this rate coefficient by

$$\tau_{m,k}^{vt}(T) = \frac{k_B T}{k_{1,0}^{m,k}(T) p [1 - \exp(-\theta_m/T)]} \quad (11)$$

a. O_2 relaxation. For the O_2–O_2 system, we have fitted the data given by Billing and Kolesnick[22] for 300 K < T < 5000 K to the following expression:

$$k_{1,0}^{O_2,O_2}(T) = 2.71 \times 10^{-8} \exp(-158.67 T^{-1/3}) \quad (12)$$

in cm^3 s^{-1}. For 300 K < T < 5000 K, the relaxation time, derived from Eq. (11), remains close to the one proposed by Millikan and White.[3] For the O_2–O system, Doroshenko et al.[20] give an analytical expression of $k_{1,0}^{O_2,O}$ for 1000 K < T < 3000 K, which is in good agreement with the one derived by Taylor.[23] Figure 2 shows that the corresponding relaxation time is shorter than the one assumed by Millikan and White, and the discrepancy increases as the temperature decreases. For the O_2–N_2, O_2–NO, and O_2–N systems, as no accurate data were available, Millikan and White's relaxation times have been used.

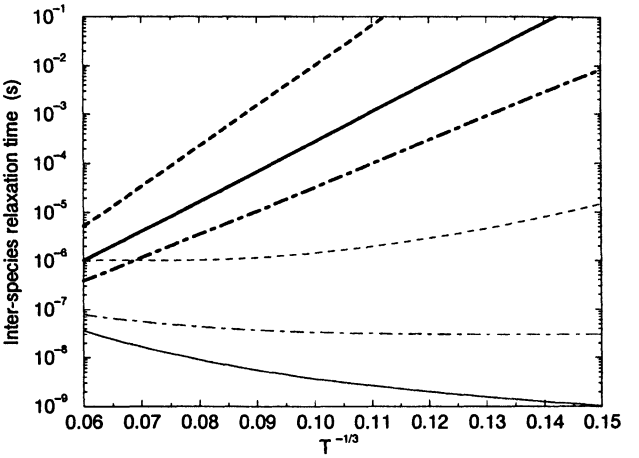

Fig. 2 *vt* relaxation times for N_2–O, NO–O, O_2–O systems at a pressure of 1 atm. ———, Doroshenko's model[20]; ———, Millikan and White's model[3]; ——, NO–O system; – – –, N_2–O system; –·–·–, O_2–O system.

b. N_2 relaxation. For the N_2–N_2 and N_2–N systems, we have used the theoretical approach proposed by Dmitrieva et al.[21] This model shows that the $T^{-1/3}$ evolution proposed by Millikan and White[3] for the N_2–N_2 relaxation time is correct down to 2000 K.[24] As already discussed in a previous study,[24] the N_2–N relaxation time estimated by Millikan and White is overestimated at high temperatures. However in this work, the N concentration remains very low in the whole flow, and therefore, this relaxation process has a negligible influence. For the N_2–O system, Doroshenko et al.[20] propose an analytical expression for $k_{1,0}^{N_2,O}(T)$, which is in good agreement with the one given by Taylor.[23] Figure 2 shows that the corresponding relaxation time, derived from Eq. (11), is much shorter than the one proposed by Millikan and White. As for the O_2–O system, the discrepancy increases as the temperature decreases. For the N_2–O_2 and N_2–NO systems, as no more accurate data were available, Millikan and White's relaxation times have been used.

c. NO relaxation. For NO–N_2 and NO–O_2 systems, the only available data in the literature are the values of $k_{1,0}^{NO,O_2}$ and $k_{1,0}^{NO,N_2}$ at 300 K. Different authors have shown that *vt* reaction rates increase with temperature. As no experimental data are available, we have assumed that over the whole temperature range of this study (300 K–4500 K), the reaction rates $k_{1,0}^{NO,O_2}$ and $k_{1,0}^{NO,N_2}$ remained constant and equal to their values at 300 K. We have retained the values given by Doroshenko et al.[20] and confirmed by Green et al.[25] This hypothesis underestimates the influence of the NO–N_2 and NO–O_2 relaxation processes, but it is more accurate than the direct use of Millikan and White's relaxation times, which are valid only at high temperatures. The influence of this hypothesis on the results will be discussed in the following sections. For the NO–O system, we have used the expression of $k_{1,0}^{NO,O}$ proposed by Doroshenko et al. for 300 K < T < 2700 K, which agrees at 300 K with the value given by Green.[25] For the NO–NO system, Doroshenko et al. give an analytical expression of $k_{1,0}^{NO,NO}(T)$ which is in good agreement with the one derived by Taylor.[23] The corresponding relaxation times of the NO–NO and NO–O systems are shorter than those proposed by Millikan and

White, and the discrepancy increases as the temperature decreases (see Fig. 2 for the NO–O system). For the NO–N system, as no more accurate data were available, Millikan and White's relaxation time has been used.

2. V–V Energy Exchange Terms

As a reference, the model (denoted as *model 1* in the following sections) proposed by Candler[26] has been used:

$$Q_{vv_m} = \sum_{r \neq m} \mathcal{N}_A \sigma_{mr} P_{mr} \sqrt{\frac{8k_B T}{\pi \mu_{mr}}} \frac{\rho_m \rho_r}{\mathcal{M}_m \mathcal{M}_r} (\bar{e}_{v_r} - \bar{e}_{v_m}) \quad (13)$$

where r and m are molecules. Candler assumed that the vv exchange probabilities P_{mr} are constant and equal to 10^{-2} for all species. However, this model is inconsistent in the sense that at thermal equilibrium ($T_{v_s} = T_{v_m} = T$), Q_{vv_m} terms are different from zero (as $\theta_m \neq \theta_r$). To eliminate this anomaly, slightly modified expressions are proposed in the literature.[27,28] In the present work, we propose to use the model (denoted as *model 2*) given by Knab et al.[27]

$$Q_{vv_m} = \sum_{r \neq m} \mathcal{N}_A \sigma_{mr} P_{mr} \sqrt{\frac{8k_B T}{\pi \mu_{mr}}} \frac{\rho_m \rho_r}{\mathcal{M}_r \mathcal{M}_m} \left(\frac{\bar{e}^{eq}_{v_m}}{\bar{e}^{eq}_{v_r}} \bar{e}_{v_r} - \bar{e}_{v_m} \right) \quad (14)$$

where $P_{mr} = 10^{-2}$ for all species. Starting from kinetic theory, other authors[29,30] derived a physically consistent model (denoted as *model 3*)

$$Q_{vv_m} = \sum_{r \neq m} \mathcal{N}_A P_{mr} v_{rm} \frac{\rho_m \rho_r}{\mathcal{M}_r \mathcal{M}_m} \times \left[\frac{1 - \exp(-\theta_m/T)}{1 - \exp(-\theta_r/T)} \frac{\bar{e}_{v_r}}{\bar{e}^{eq}_{v_r}} (\bar{e}^{eq}_{v_m} - \bar{e}_{v_m}) - \frac{\bar{e}_{v_m}}{\bar{e}^{eq}_{v_r}} (\bar{e}^{eq}_{v_r} - \bar{e}_{v_r}) \right] \quad (15)$$

with

$$v_{rm} = \sqrt{\frac{8k_B T}{\pi \mu_{mr}}} \frac{\pi (d_m + d_r)^2}{4} \quad (16)$$

As expected, with this formulation, Q_{vv_m} terms vanish at thermal equilibrium. For vv exchange probabilities, two sets have been tested: first, as a reference, we have used model 3, assuming that $P_{mr} = 10^{-2}$. Then, we have tried to determine in the literature the best possible data for vv exchange probabilities. For 500 K < T < 3000 K, Park and Lee[19] fit the probabilities measured by Taylor et al.[31] for the N_2–O_2 and N_2–NO systems. For the O_2–NO system, Park and Lee proposed to take the same probability as the N_2–NO system. Figure 3 shows that these probabilities increase with temperature but remain much less than 10^{-2}. We have compared these data with the probabilities derived from the studies of Doroshenko et al.[20] and Makarov[30] for the N_2–O_2 and N_2–NO systems. Unfortunately, no accurate data are available on the O_2–NO system. Figure 3 shows that significant discrepancies exist between the models, but for all systems the probabilities remain less than 10^{-2} over the temperature range 300–5000 K. Finally, in this work, we propose to test model 3 with a second set for vv exchange probabilities, using the fitting laws proposed by Park and Lee.[19]

3. Chemical–Vibrational Energy Exchange Terms

In numerous studies, the vibrational energy transfer for molecule m caused by chemical reactions is written

$$Q_{cv_m} = \dot{w}_m e_{v_m} \quad (17)$$

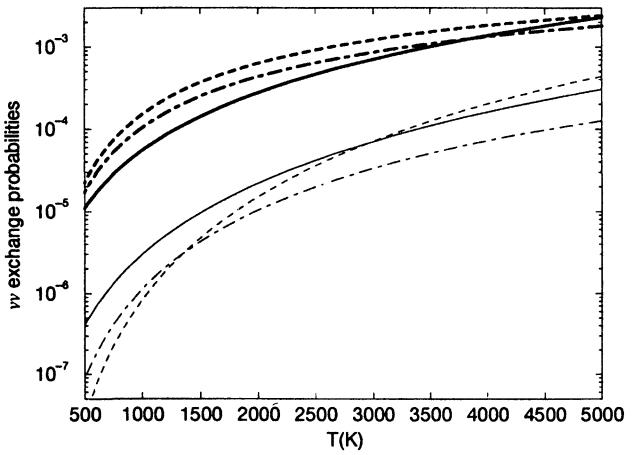

Fig. 3 vv exchange probabilities for N_2–O_2 and N_2–NO systems. ———, N_2–O_2 system; ———, N_2–NO system; ——, Park and Lee's fitting laws[19]; – – –, Doroshenko's values[20]; –·–·–, Makarov's values.[30]

Knab et al.[17,27] pointed out that this approach is inconsistent in the sense that it does not take into account the following facts:

1) The C–V energy transfer must not be modeled independently of the nonequilibrium reaction rate constants.

2) The average vibrational energies gained $G_{\text{app},mj}$ or lost $G_{va,mj}$ by a molecule m being created or destroyed in a reaction j differ from each other at thermal nonequilibrium.

These authors proposed a consistent approach, as denoted by the CVCV model. This approach gives

$$Q_{cv_m} = \sum_{j=1}^{5} (\dot{w}_{\text{app},mj} G_{\text{app},mj} - \dot{w}_{va,mj} G_{va,mj}) \quad (18)$$

where j is a chemical reaction. Further details may be found in Ref. 17 and references within. In this study, we propose to test the influence of both approaches on the results.

V. Results and Discussion

Figures 4 and 5 show axial evolutions of the pressure and of the x-component velocity on the nozzle axis. We have noted a very small influence of the models used for the kinetic scheme and the energy exchange terms on these axial profiles. Figures 4 and 5 show that our results are in close agreement with those obtained by Tumino et al.[2] on the nozzle axis. We have also observed a good agreement on radial profiles where the discrepancy between both studies remains less than 10%. In the first centimeters of the diverging region ($x > 0$), the expansion of the jet is very strong, but there is a recompression zone at $x \simeq 0.55$ m, which is caused by the shape of the nozzle. Downstream, the pressure is uniform. Figure 5 shows that the velocity increases rapidly in the converging region and in the first centimeters of the diverging part, and is uniform for $x > 0.6$ m. The computation of the freejet downstream of the nozzle exit has shown that the flow conditions on the flow axis remain unchanged between the nozzle exit and the test section located 170 mm downstream. Therefore, in this study, we have carried out a comparison between computations and experiments at the nozzle exit. Figure 5 shows that the calculated velocity is slightly less than the measured one (3300 ± 200 m/s). The latter is closer to the velocity calculated assuming that the flow is in full thermal and chemical equilibrium.

Figures 6–10 show the axial translational and vibrational temperatures calculated with different energy exchange models. In their study, Tumino et al.[2] considered only one average vibrational temperature. In this work, we test the influence of a more accurate modeling of the nonequilibrium of the flow. First, it is interesting to note that the choice of Park or Losev's

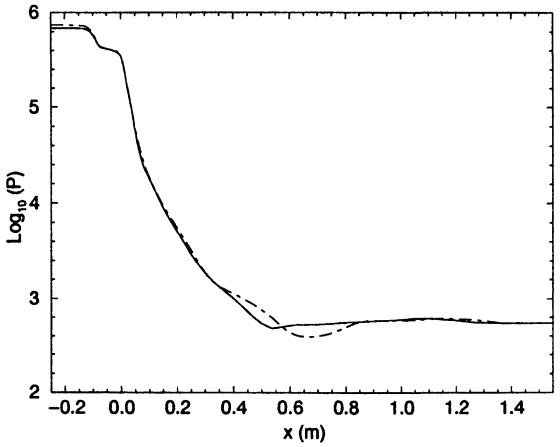

Fig. 4 Pressure on the nozzle axis. ——, present study; – · – · –, Tumino et al.[2]

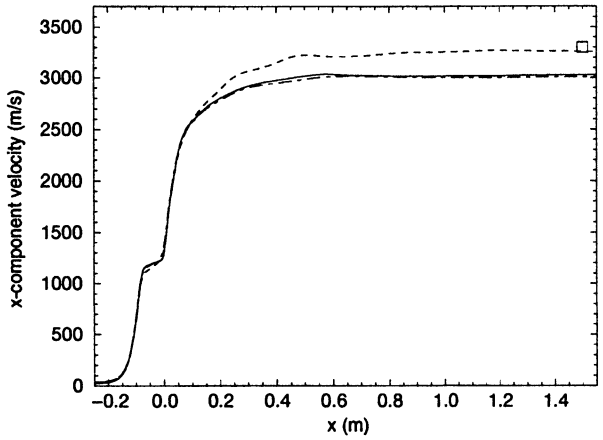

Fig. 5 Velocity on the nozzle axis. ——, present study; – · – · –, Tumino et al.[2]; – – –, full equilibrium flow; □, measurement.

model for the rate coefficients, and the choice of the consistent CVCV model or the one-temperature model and Eq. (17) have only a small influence on the temperatures. As observed by Tumino et al., we have also noted that wall conditions have only a very small influence on the temperatures calculated on the nozzle axis.

Figure 6 shows the axial temperatures calculated with Millikan and White's[3] relaxation times for V–T exchanges, and model 1 for the V–V term with all vv exchange probabilities equal to 10^{-2}. With these widely used models, we note that in the converging part of the nozzle ($x < 0$), where the pressure is high enough to ensure that the flow is in full equilibrium, the calculated vibrational temperatures remain different from the translational one. This results from the inconsistency of model 1 for the V–V energy exchange term. In the diverging region of the nozzle ($x > 0$), the three vibrational temperatures remain close to each other and are much higher than the translational temperature. The calculated flow appears to be in strong thermal nonequilibrium. We note that the translational temperature is very close to the one calculated by Tumino et al. in considering only one average vibrational temperature.

Figure 7 shows the axial temperatures calculated with the same model as Fig. 1 for V–V exchanges and Doroshenko's model for V–T relaxation times. As the M–O V–T relaxation times are much shorter in Doroshenko's model than in Millikan and White's model, the calculated vibrational temperatures in the diverging part of the nozzle are much closer to the translational one in Fig. 7 than in Fig. 6. In the diverging region, the translational temperature is increased, and is about 200 K higher at the nozzle exit than in Fig. 6.

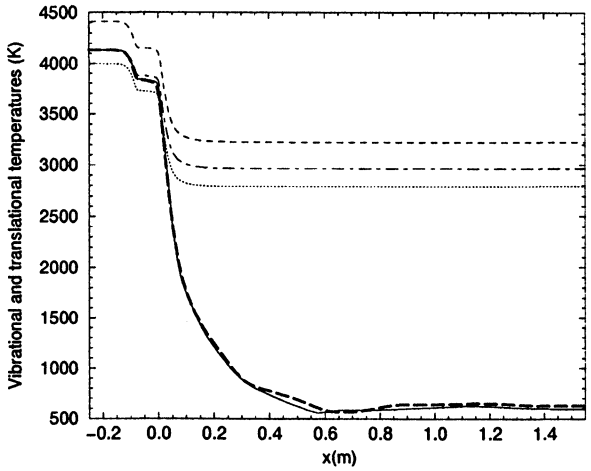

Fig. 6 Vibrational and translational temperatures on the nozzle axis with Millikan and White's model[3] for V–T relaxation times, and model 1 for the V–V term with vv exchange probabilities equal to 10^{-2} for all species. ——, translational temperature; — — — —, translational temperature calculated by Tumino et al.[2]; – – –, T_{v,N_2}; · · · · · ·, T_{v,O_2}; – · – · –, $T_{v,NO}$.

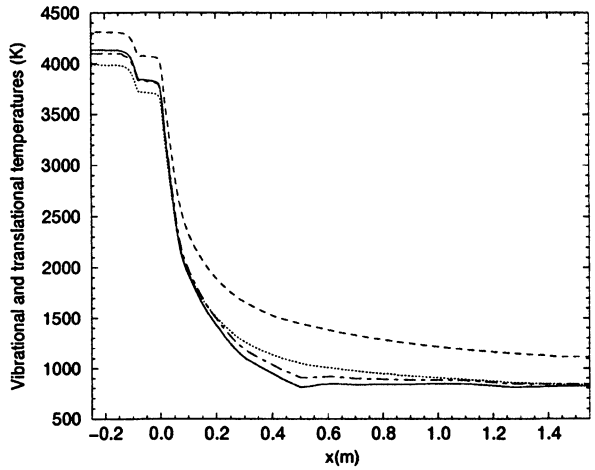

Fig. 7 Vibrational and translational temperatures on the nozzle axis with Doroshenko's model[20] for V–T relaxation times, and model 1 for the V–V term with vv exchange probabilities equal to 10^{-2} for all species. ——, translational temperature; – – –, T_{v,N_2}; · · · · ·, T_{v,O_2}; – · – · –, $T_{v,NO}$.

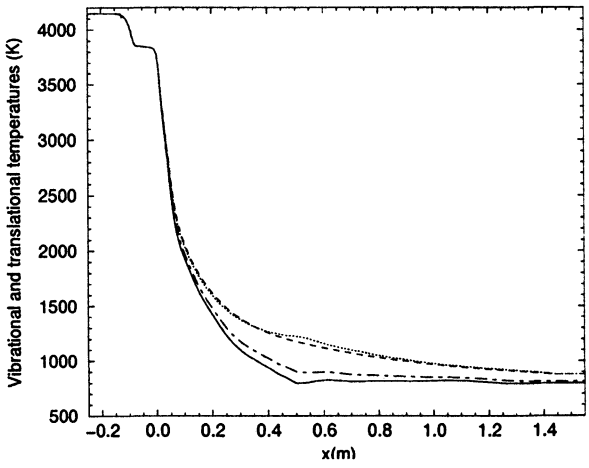

Fig. 8 Vibrational and translational temperatures on the nozzle axis with Doroshenko's model[20] for V–T relaxation times, and model 2 for the V–V term with vv exchange probabilities equal to 10^{-2} for all species. ——, translational temperature; – – –, T_{v,N_2}; · · · · ·, T_{v,O_2}; – · – · –, $T_{v,NO}$.

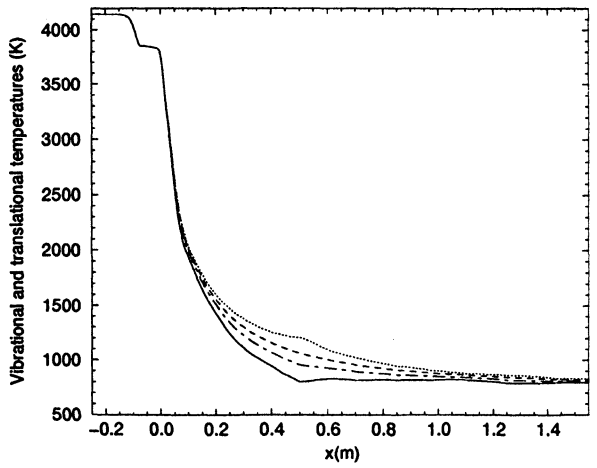

Fig. 9 Vibrational and translational temperatures on the nozzle axis with Doroshenko's model[20] for V–T relaxation times, and model 3 for the V–V term with *vv* exchange probabilities equal to 10^{-2} for all species. ——, translational temperature; – – –, T_{v,N_2}; · · · · ·, T_{v,O_2}; – · – · –, $T_{v,NO}$.

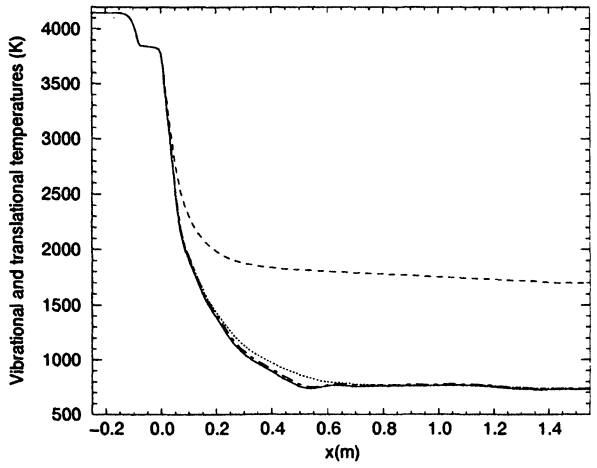

Fig. 10 Vibrational and translational temperatures on the nozzle axis with Doroshenko's model[20] for V–T relaxation times, and model 3 for the V–V term with the *vv* exchange probabilities fitted by Park and Lee.[19] ——, translational temperature; – – –, T_{v,N_2}; · · · · ·, T_{v,O_2}; – · – · –, $T_{v,NO}$.

Figures 8 and 9 show the axial temperatures calculated with Doroshenko's model for V–T relaxation times, and models 2 and 3, respectively, for the V–V term with all *vv* exchange probabilities equal to 10^{-2}. In the converging part of the nozzle, as expected, models 2 and 3 correct efficiently model 1, and the calculated flow is in thermal equilibrium. We note that the V–V energy exchange model also affects the vibrational temperatures calculated in the diverging region but has no influence on the translational temperature.

Figure 10 is the same as Fig. 9 but with the fitting laws proposed by Park and Lee[19] for *vv* exchange probabilities. In this case, in the diverging part of the nozzle $T_{v_{NO}} \simeq T_{v_{O_2}} \simeq T$, whereas $T_{v_{N_2}}$ remains higher.

Figures 9 and 10 clearly show that assuming that all *vv* exchange probabilities are constant and equal to 10^{-2} significantly overestimates the influence of the V–V coupling. In our flow conditions, these figures show that V–T relaxation processes are much more efficient than the V–V ones. As mentioned in Sec. IV.B.*1*, NO–N_2 and NO–O_2 relaxation times are certainly overestimated in Doroshenko's model. However, in our conditions, the NO–O relaxation process is efficient enough to ensure $T_{v_{NO}} \simeq T$. Therefore, a more accurate modeling of these two relaxation times is not necessary.

Figures 6–10 have clearly pointed out the significant influence of the energy exchange terms on the calculated temperatures, and therefore, the necessity of an accurate modeling of these terms. Experimentally, the rotational temperature of NO has been measured at the nozzle exit. As relaxation processes are well known to be very efficient for the NO molecule, the measured temperature can be considered to be equal to the translational temperature. Figures 6 and 10 show that the calculated translational temperature at the nozzle exit is only slightly increased when state-of-the-art models for V–V and V–T exchanges are used, and remains less than the measured one (1200 ± 200 K). It is interesting to note that the temperature calculated, assuming that the flow is in thermochemical equilibrium, is 1550 K at the nozzle exit.

Figure 11 shows axial species mass fractions calculated with Park's model. As observed for temperatures, we have noted that, whatever the wall catalycity, wall conditions have a negligible influence on the axial evolutions of species mass fractions. In Fig. 11, all mass fractions are rapidly frozen in the diverging part of the nozzle to values far from equilibrium, with, in particular, a high concentration of O and NO species.

Figure 12 compares the NO number density calculated at the nozzle exit with Park or Losev's models with the measured one. The accuracy of the latter is difficult to estimate but certainly remains within a factor of 5. We note that both models overestimate by more than one order of magnitude the NO concentration at the nozzle exit. Despite the differences be-

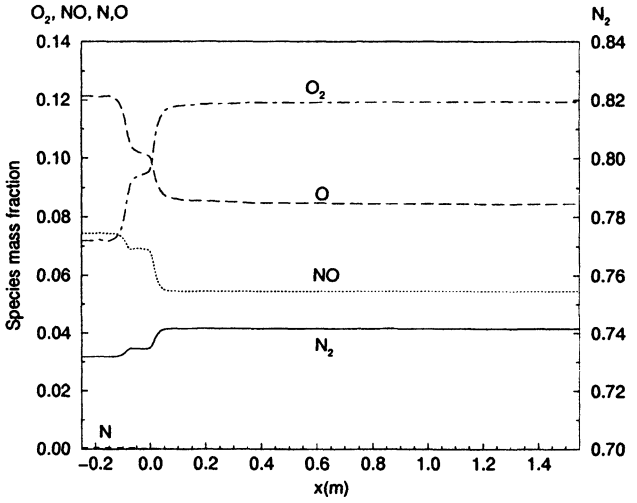

Fig. 11 Species mass fractions on the nozzle axis calculated with Park's model[15] for the reaction rates.

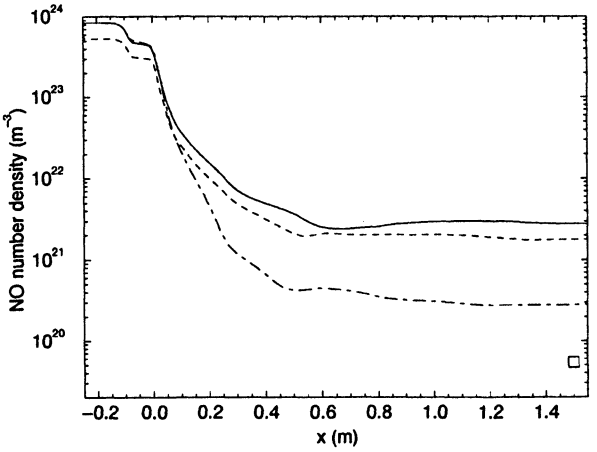

Fig. 12 Comparison of the measured NO number density (square) on the nozzle axis with those computed using different models for reaction rates. ——, Park's model[15]; – – –, Losev's model[16]; – · – · –, full equilibrium flow.

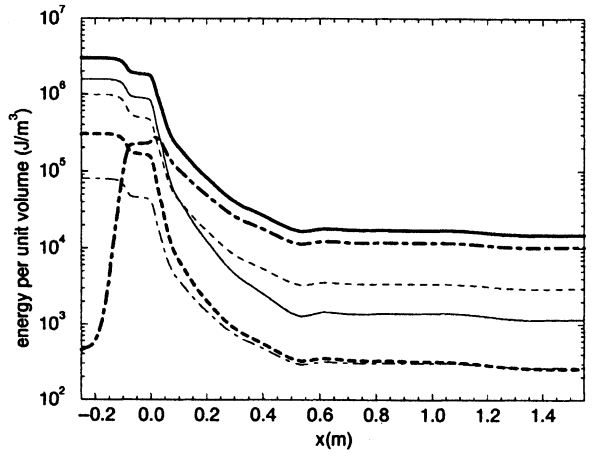

Fig. 13 Energy distribution on the nozzle axis. ——, ρe_t; —·—·—, ρe_c; — — —, $\rho_{N_2} e_{v,N_2}$; ——, $\rho c_v T$; -·-·-, $\rho_{NO} h^0_{NO}$; - - -, $\rho_O h^0_O$.

fjtween Park and Losev's reaction rates, Fig. 12 shows that the NO number density calculated with Losev's model is only slightly less than the one calculated with Park's model. Other reaction rate values of the literature have been tested, in particular for exchange reactions,[19,32,33] but no significant improvement has been observed. It is important to note that the model used for the vibration–chemistry coupling has a negligible influence on the profiles of Figs. 11 and 12. Finally, in Fig. 12, we have represented the NO density calculated when one assumes that the flow is in full equilibrium (with Park's reaction rates). In this case, the agreement with experiment is significantly improved.

To better understand the reasons of the significant discrepancies between computations and experiments, in Fig. 13, the axial evolution of the total energy of the flow ρe_t [Eq. (5)] and the contribution of the five most significant terms, namely, ρe_c, $\rho c_v T$, $\rho_O h^0_O$, $\rho_{N_2} e_{v_{N_2}}$, and $\rho_{NO} h^0_{NO}$ for the conditions of Fig. 10 and Losev's model, have been represented. In the converging part of the nozzle, the kinetic energy is negligible and the energy of the flow is mainly contained in the translational energy of the gas and in the energy of formation of O atoms. This distribution of energy changes in the diverging region where the kinetic energy is the most significant contribution to the total energy, and $\rho c_v T$ and $\rho_{NO} h^0_O$ are much smaller. We note that in this nozzle flow, the energy contained in the vibrational modes remains small.

Figure 13 clearly shows that inlet conditions have a very strong influence on the flowfield calculated at the nozzle exit. Therefore, inlet conditions must be determined very accurately. Measurement methods of the mass flow rate and the electric power are reliable, then the values given in Sec. II.C can be considered to be accurate. Conversely, the accuracy of T_0 is much more difficult to estimate. This temperature corresponds to a total specific enthalpy (derived assuming a chemical equilibrium) of 7 MJ kg^{-1}. Considering the air mass flow rate is 0.5 kg s^{-1} and the arcjet electric power supply is 4 MW, we obtain an energy transfer efficiency of 90%, which is rather optimistic. For the same mass flow rate, assuming a lower efficiency would result in a lower T_0, and therefore, a higher discrepancy between computations and experiments at the nozzle exit for the translational temperature. To attempt to improve the experiment/modeling agreement, we have carried out computations with slightly different inlet conditions. We have noted that the calculated velocity and translational temperature at the nozzle exit depend mainly on T_0 and weakly on P_0, and that the calculated NO number density at the nozzle exit decreases as T_0 increases and decreases with P_0. However, even with deviations of 10 or 20% from current inlet conditions, the agreement between calculated and measured T, u, and NO number density is not significantly increased.

Finally, it is important to note that the concentration of copper has been measured in the flow and is 3.6×10^{-3}% in mass (17 ppm). To our knowledge, only few numerical and experimental works[6,19,34] have been devoted to the study of contamination effects in air nozzle flows. However, all of these studies indicate that up to a concentration of several hundreds of particles per million, the presence of copper has a negligible influence on the flow. In fact, a thorough study of contamination effects in the TT1 nozzle flow would be of great interest, but the contamination of the flow seems to be too low to significantly modify the species concentrations, and therefore to explain the NO number density measured at the nozzle exit.

VI. Conclusions

The modeling of a nonequilibrium supersonic air nozzle flow has been carried out and compared with measurements at the nozzle exit. Different models for the kinetic scheme, V–T, V–V, and C–V energy exchange terms have been discussed and tested. In this study, the choice of the kinetic scheme and the modeling of the C–V energy exchange terms have only a small influence on the calculated flow. Conversely, V–V and V–T couplings significantly affect the calculated temperatures in the nozzle. This study has clearly put forward the necessity of an accurate modeling of these energy exchange terms. For the V–T relaxation times, the widely used analytical expressions proposed by Millikan and White[3] are well known to overestimate the relaxation times when the molecule is NO or the colliding species is an atom. In this study, we have used a set of relaxation times based on the best possible data available in the literature. For the V–V term, we have first put forward the necessity to use a consistent model (denoted model 3 in this work). Then, we have shown that assuming that all *vv* exchange probabilities were constant and equal to 10^{-2} strongly overestimates the efficiency of the V–V coupling. Currently, significant discrepancies exist between the values of *vv* exchange probabilities given in the literature. However, all studies indicate that for 300 K $< T <$ 5000 K, these probabilities increase with temperature and remain much less than 10^{-2}. In this work, we have used the fitting laws given by Park and Lee.[19]

Finally, a fairly good experiment/modeling agreement is obtained on velocity, but computations underestimate by about 30% the translational temperature and overestimate by more than one order of magnitude the NO number density at the nozzle exit. As observed in the study of the F4 hot-shot wind tunnel,[6] in the TT1 facility the experimental results are much closer to the values calculated, assuming that the flow is in full equilibrium. Finally, to improve the experiment/modeling agreement, complementary measurements would be of great interest at the nozzle exit, e.g., O number density, and in the arc chamber, where the accuracy of current data is difficult to estimate.

Acknowledgments

The authors would like to thank L. Robin for his helpful explanations on the measurements he carried out at the TT1 facility, and also L. Marraffa and G. Tumino from the European Space Research and Technology Centre, Noordwijk, The Netherlands, for providing us numerical results to compare with ours. Calculation facilities have been provided by the Institut de Développement et des Ressources en Informatique Scientifique and the Centre de Ressources Informatiques de Haute-Normandie.

References

[1]Robin, L., Honoré, D., and Vervisch, P., "Laser-Induced Fluorescence Measurements in High-Enthalpy Facilities: Application to the Study of Air Plasma/Surface Interaction," *Proceedings of the 20th International Symposium on Shock Waves* (Pasadena, CA), World Scientific Publishing Co., 1995, pp. 269–274.

[2]Tumino, G., Marraffa, L., Robin, L., Durand, G., and Tribot, J. P.,

"Computational Analysis of LIF Measurements in TT1 Arc-Jet Facility," 15th IMACS World Congress on Scientific Computation, Modelling and Applied Mathematics, Berlin, Aug. 1997.

[3]Millikan, R. C., and White, D. R., "Systematics of Vibrational Relaxation," *Journal of Chemical Physics*, Vol. 39, No. 12, 1963, pp. 3209–3213.

[4]Dunn, M. G., and Kang, S. W., "Theoretical and Experimental Studies of Reentry Plasmas," NASA CR 2232, 1973.

[5]Park, C., "Assessment of Two-Temperature Kinetic Model for Ionizing Air," AIAA Paper 87-1574, June 1987.

[6]Sagnier, P., Vérant, J. L., Devezeaux, D., Masson, A., and Mohamed, A. K. "Comparison Between Measurements and Modelings in the ONERA F4 Hot Shot Wind Tunnel," 87th Supersonic Tunnel Association Meeting, Modane, France, May 1997.

[7]Lee, J. H., "Basic Governing Equations for the Flight Regimes of Aeroassisted Orbital Transfer Vehicles," AIAA Paper 84-1729, June 1984.

[8]Harten, A., "High Resolution Scheme for Hyperbolic Conservation Laws," *Journal of Computational Physics*, Vol. 49, 1983, pp. 357–393.

[9]Bourdon, A., and Vervisch, P., "Study of a Low-Pressure Nitrogen Plasma Boundary Layer over a Metallic Plate," *Physics of Plasmas*, Vol. 4, No. 11, 1997, pp. 4144–4157.

[10]Wilke, C. R., "A Viscosity Equation for Gas Mixtures," *Journal of Chemical Physics*, Vol. 18, No. 4, 1950, pp. 517–519.

[11]Gupta, R. N., Yos, J. M., Thompson, R. A., and Lee, K. P., "A Review of Reaction Rates and Transport Properties for an 11-Species Air Model for Chemical and Thermal Nonequilibrium Calculations to 30,000 K," NASA RP-1232, Aug. 1990.

[12]Mason, E. A., and Saxena, S. C., "Approximate Formula for the Thermal Conductivity of Gas Mixtures," *Physics of Fluids*, Vol. 1, No. 5, 1958, pp. 361–369.

[13]Anderson, J. D., *Hypersonic and High Temperature Gas Dynamics*, McGraw–Hill, New York, 1989.

[14]Ramshaw, J. D., "Self-Consistent Effective Binary Diffusion in Multicomponent Gas Mixtures," *Journal of Non-Equilibrium Thermodynamics*, Vol. 15, No. 3, 1990, pp. 295–300.

[15]Park, C., "A Review of Reaction Rates in High Temperature Air," AIAA Paper 89-1740, June 1989.

[16]Krivonosova, O. E., Losev, S. A., Nalivaiko, V. P., Mukoseev, Y. K., and Shatalov, O. P., "Recommended Data on the Rate Constants of Chemical Reactions Among Molecules Consisting of N and O Atoms," *Reviews of Plasma Chemistry*, Vol. 1, 1991, pp. 1–29.

[17]Knab, O., Frühauf, H. H., and Messerschmid, E. W., "Theory and Validation of the Physically Consistent Coupled Vibration-Chemistry-Vibration Model," *Journal of Thermophysics and Heat Transfer*, Vol. 9, No. 2, 1995, pp. 219–226.

[18]Treanor, C. E., and Marrone, P. V., "Effect of Dissociation on the Rate of Vibrational Relaxation," *Physics of Fluids*, Vol. 5, No. 9, 1962, pp. 1022–1026.

[19]Park, C., and Lee, S. H., "Validation of Multitemperature Nozzle Flow Code," *Journal of Thermophysics and Heat Transfer*, Vol. 9, No. 1, 1995, pp. 9–16.

[20]Doroshenko, V. M., Kudryavtsev, N. N., and Smetanin, V. V., "Equilibrium of Internal Degrees of Freedom of Molecules and Atoms in Hypersonic Flight in the Upper Atmosphere," *High Temperature* (translated from *Teplofizika Vysokikh Temperatur*), Vol. 29, No. 5, 1991, pp. 1013–1027.

[21]Dmitrieva, I. K., Pogrebnya, S. K., and Porshnev, P. I., "V-T and V-V Rate Constants for Energy Transfer in Diatomics. An Accurate Analytical Approximation," *Chemical Physics*, Vol. 142, 1990, pp. 25–33.

[22]Billing, G. D., and Kolesnick, R. E., "Vibrational Relaxation of Oxygen. State to State Rate Constants," *Chemical Physics Letters*, Vol. 200, No. 4, 1992, pp. 382–386.

[23]Taylor, R. L., "Energy Transfer Processes in the Stratosphere," *Canadian Journal of Chemistry*, Vol. 52, 1974, pp. 1436–1451.

[24]Domingo, P., Bourdon, A., and Vervisch, P., "Study of a Low Pressure Nitrogen Plasma Jet," *Physics of Plasmas*, Vol. 2, No. 7, 1995, pp. 2853–2862.

[25]Green, B. D., Caledonia, G. E., Murphy, R. E., and Robert, F. X., "The Vibrational Relaxation of NO(v = 1 − 7) by O_2," *Journal of Chemical Physics*, Vol. 76, No. 5, 1982, pp. 2441–2448.

[26]Candler, G. V., "The Computation of Weakly Ionized Hypersonic Flows in Thermo-Chemical Nonequilibrium," Ph.D. Dissertation, Stanford Univ., Stanford, CA, 1988.

[27]Knab, O., Frühauf, H. H., and Messerschmid, E. W., "URANUS/CVCV Model Validation by Means of Thermochemical Nonequilibrium Nozzle Airflow Calculations," *Proceedings of the 2nd European Symposium on Aerothermodynamics for Space Vehicles*, ESA Publications Div., Noordwijk, The Netherlands, 1994, pp. 129–134.

[28]Candler, G. V., and MacCormack, R. W., "Computation of Weakly Ionized Hypersonic Flows in Thermochemical Nonequilibrium," *Journal of Thermophysics and Heat Transfer*, Vol. 5, No. 3, 1991, pp. 266–273.

[29]Candel, S., Thivet, F., and Perrin, M. Y., "A Unified Nonequilibrium Model for Hypersonic Flows," *Physics of Fluids A*, Vol. 3, No. 11, 1991, pp. 2799–2812.

[30]Makarov, V. N., "The Kinetics of Physicochemical Processes in High-Temperature Air," *High Temperature* (translated from *Teplofizika Vysokikh Temperatur*), Vol. 33, No. 4, 1995, pp. 583–587.

[31]Taylor, R. L., Camac, M., and Feinberg, R. M., "Measurements of Vibration-Vibration Energy Coupling in Gas Mixtures," *Proceedings of the 11th Symposium (International) on Combustion*, The Combustion Inst., Pittsburgh, PA, 1967, pp. 49–65.

[32]Kossyi, A., Kostinsky, A. Y., Matveyev, A. A., and Silakov, V. P., "Kinetic Scheme of the Nonequilibrium Discharge in Nitrogen-Oxygen Mixtures," *Plasma Sources Science and Technology*, Vol. 1, No. 3, 1992, pp. 207–220.

[33]Bose, D., and Candler, G., V., "Kinetics of the $N_2 + O \rightarrow NO + N$ Reaction Under Thermodynamic Nonequilibrium," *Journal of Thermophysics and Heat Transfer*, Vol. 10, No. 1, 1996, pp. 148–154.

[34]Pietre, S., and Netterfield, M. P., "Navier-Stokes Computations for High Enthalpy Nozzle Flows, Including Contamination Effects," AIAA Paper 94-1997, June 1994.